Available online at www.sciencedirect.com
ScienceDirect
Composite Structures 76 (2006) 88–93
COMPOSITE STRUCTURES
www.elsevier.com/locate/compstruct

Mode II fracture behaviour monitoring for composite laminates using embedded fibre Bragg grating sensors

Hang-yin Ling [a,*], Kin-tak Lau [a], Li Cheng [a], Zhongqing Su [a,b]

[a] Department of Mechanical Engineering, The Hong Kong Polytechnic University, Hong Kong, China
[b] Laboratory of Smart Materials and Structures (LSMS), Centre for Advanced Materials Technology (CAMT), School of Aerospace, Mechanical and Mechatronic Engineering, The University of Sydney, NSW 2006, Australia

Abstract

This paper presents the utility of embedded fibre Bragg grating (FBG) sensors for monitoring mode II fracture behaviour of glass fibre-reinforced epoxy (GF/EP) composite beams bearing a mid-plane delamination. Stress concentration at the delamination tip of the beam, induced during an end notched flexure (ENF) test, was monitored by means of the reflection spectrum obtained from the FBG sensor whose centre was located at the tip of delamination. The Bragg wavelength shift, bandwidth and intensity in such a reflection spectrum associated with a load–displacement graph were then used to characterize the fracture behaviour of the delaminated beam.

Keywords: Delamination; Mode II; ENF test; Stress concentration; Embedded optical fibre sensor; Fibre Bragg grating (FBG) sensor

1. Introduction

Advanced composite materials have been widely utilized in marine, aerospace and automotive sectors owing to their superior properties such as comparably high strength-to-weight ratio and excellence in corrosion resistance. Since compressive strength of composite structures would be significantly decreased because of appearance of delamination, it is necessary to study the fracture behaviour of the defective composite structures such that the defect in the structure can be effectively monitored, so as to ensure the structural integrity during their service life.

The need of a real-time structural health monitoring (SHM) in the composite structures has motivated the development of smart composite structures in the past few years [1–3]. The smart composite structures generally consist of some distributed surface bonded or embedded sensors and actuators, and one or more microprocessors that are able to analyze the responses from the sensors and use integrated control theory to command the actuators to alter system response. In particular, fibre Bragg grating (FBG) sensors have been increasingly adopted in this area since their emergence, acting as an intrinsic smart sensor for their attractive advantages such as lightweight, small in size, good performance under harsh environmental conditions, multiplexing ability and exemption from electromagnetic inference.

An extensive investigation on using embedded FBG sensors for delamination monitoring in the composite structures has been reported [4–8]. In static loading cases, a FBG sensor was employed to identify the presence of delamination under a three-point bending test in virtue of the change in the flexural strain [4]. Ling et al. [5] demonstrated a delamination detection scheme for composite structures in conjunction with a genetic algorithm by calibrating the shift in structural natural frequencies obtained from FBG sensors. By analyzing a reflection spectrum from the FBG sensors, Takeda et al. [6–8] have revealed that the reflection spectrum from the FBG sensor is very sensitive to the growth and the size of delamination under four-point bending and cyclic loading tests, which can be

* Corresponding author.
E-mail address: carrie.lhy@alumni.polyu.edu.hk (H.-y. Ling).

0263-8223/$ - see front matter © 2006 Published by Elsevier Ltd.
doi:10.1016/j.compstruct.2006.06.013

qualitatively characterized by the change in the reflection spectrum such as the Bragg wavelength shift, the bandwidth, the intensity or the presence of multiple peaks.

Inspired by the lack of study focusing on the exploitation of the embedded FBG sensors for monitoring the mode II fracture behaviour of composite laminates, the use of embedded FBG sensors for this propose in glass fibre-reinforced epoxy (GF/EP) composite beams is introduced in the present work. An end notched flexure (ENF) test is applied for studying the fracture behaviour of a composite beam containing a mid-plane delamination on the basis of a reflection spectrum obtained from the FBG sensors. By locating the FBG sensors at the tip of delamination, the strain variation due to stress concentration at the delamination tip can be evaluated. Associated with a load–displacement graph, the relationship between the reflection spectrum and the fracture behaviour of the beams is then established.

2. Principle of FBG sensor

Principle of a fibre Bragg grating (FBG) sensor for monitoring the mode II facture behaviour of composite laminates originates from stress concentration of the FBG sensor at the delamination tip. The FBG sensor, fabricated by UV irradiation of the fibre via a "phase mask technique", is a permanent periodic modulation in the index of refraction along a given length of the optical fibre core [9]. Fig. 1(a) and (b) show the refractive index variation along the gauge length of a uniform FBG and its reflection spectrum, respectively. Bragg wavelength (λ_B, wavelength at maximum reflectivity) and bandwidth ($\bar{\lambda}$, distance between the two first minima) are two characteristic parameters of the reflection spectrum. Both of them can be adjusted by changing the parameters of the grating during the writing process. According to the Bragg's law, λ_B, is given by

$$\lambda_B = 2n_{\text{eff}}\Lambda \tag{1a}$$

and

$$\frac{\bar{\lambda}}{\lambda_B} = \frac{2\Lambda}{L} \tag{1b}$$

where Λ is a grating period, L is the gauge length and n_{eff} is an effective mode index of refraction.

When a uniform strain is applied along the grating, the reflection spectrum shifts keeping its original narrow shape, for the fact that the grating period and effective mode index of refraction are also uniformly changed along the entire gauge length. However, the shape of the reflection spectrum can be changed dramatically in an unpredictable manner when the grating is subjected to a non-uniform strain along the longitudinal direction. As the shape of the reflection spectrum strongly depends on the applied non-uniform strain [10], it is possible to monitor the whole fracture process of the composite laminates by examining the variation of reflection spectrum obtained from the FBG sensor centralized at the delamination tip. The change of the strain distribution along the grating can thus be potentially used to surveil the process of the delamination growth in the composite laminates.

For a grating subjected to the non-uniform strain, $\varepsilon_{xx}(x)$, along the grating direction (x-direction), can be associated with the grating period as

$$\Lambda(x) = \Lambda_0(1 + \varepsilon_{xx}(x)) \tag{2}$$

and Eq. (1a) becomes,

$$\lambda_B(x) = 2n_{\text{eff}}(x)\Lambda(x) = 2n_{\text{eff}\,0}\Lambda_0(1 + \varepsilon_{xx}(x)) \tag{3}$$

where Λ_0 and $n_{\text{eff}\,0}$ are an initial grating period and an initial average effective mode index of refraction at the strain-free state. Eq. (3) implies that the Bragg wavelength varies with the non-uniform strain resulted in a distortion of the reflection spectrum.

3. Experimental study

Stress concentration around the tip of the delamination in a GF/EP composite beam, can be characterized by the FBG sensor under an ENF test. To this end, balanced type woven glass fibre composite laminates with a stacking sequence of $[0°]_{10}$ were fabricated by a hand lay-up process. To simulate a mid-plane delamination taken place in the composite laminates, a thin Telfon film was inserted between the 5th and 6th laminate layers during the fabrication process. Then, a rectangular ENF specimen with a

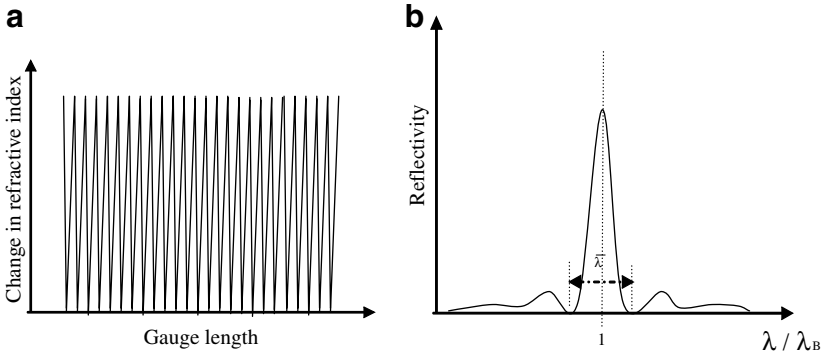

Fig. 1. (a) Refractive index variation along the gauge length of a uniform FBG, (b) corresponding reflection spectrum from a uniform FBG.

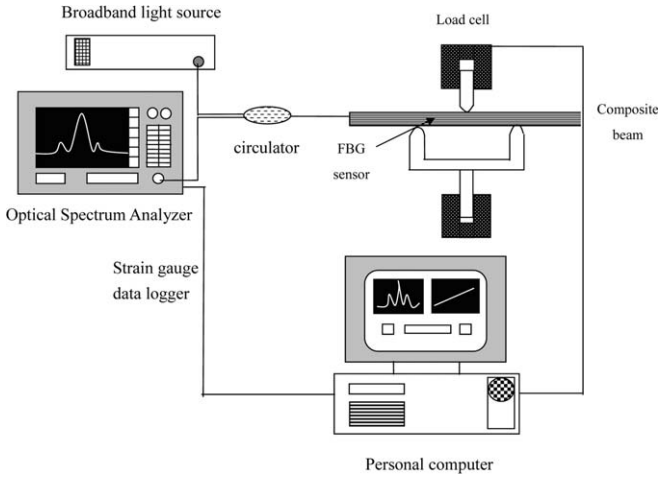

Fig. 2. Schematic diagram of whole data acquisition system in the ENF test.

dimension of 160 mm × 25 mm × 2 mm was shaped from the composite laminates. Single mode FBG sensors, 10 mm in length, 250 μm and 125 μm in coating and cladding diameters, respectively, were embedded between the top two layers of the samples. Two samples, an intact beam and a delaminated specimen with a 5.5 cm edged delamination located at the mid-plane, were tested to evaluate the effects of the delamination on a reflection spectrum from the FBG sensor. It is important to note that the centre of the FBG sensor was located at the tip of delamination in order to capture the non-uniform strain distribution around the delamination tip during the fracture process of the specimen. For the intact sample, the FBG sensor was positioned at the same location as the delaminated one.

All the tests were conducted using a MTS static axial loading test machine. The specimens were loaded under a constant displacement rate of 1 mm/min, the strain variation was recorded by the FBG sensor in every extension interval at 0.5 mm and a reflection spectrum from the FBG sensor was simultaneously obtained using an optical spectrum analyzer (OSA). Furthermore, the load–displacement relationship was established by a build-in load cell of the test machine with a maximal recordable load of 50 kN. The tests were stopped when the beams were totally fractured. A schematic diagram of a whole data acquisition system in this experiment is sketched in Fig. 2.

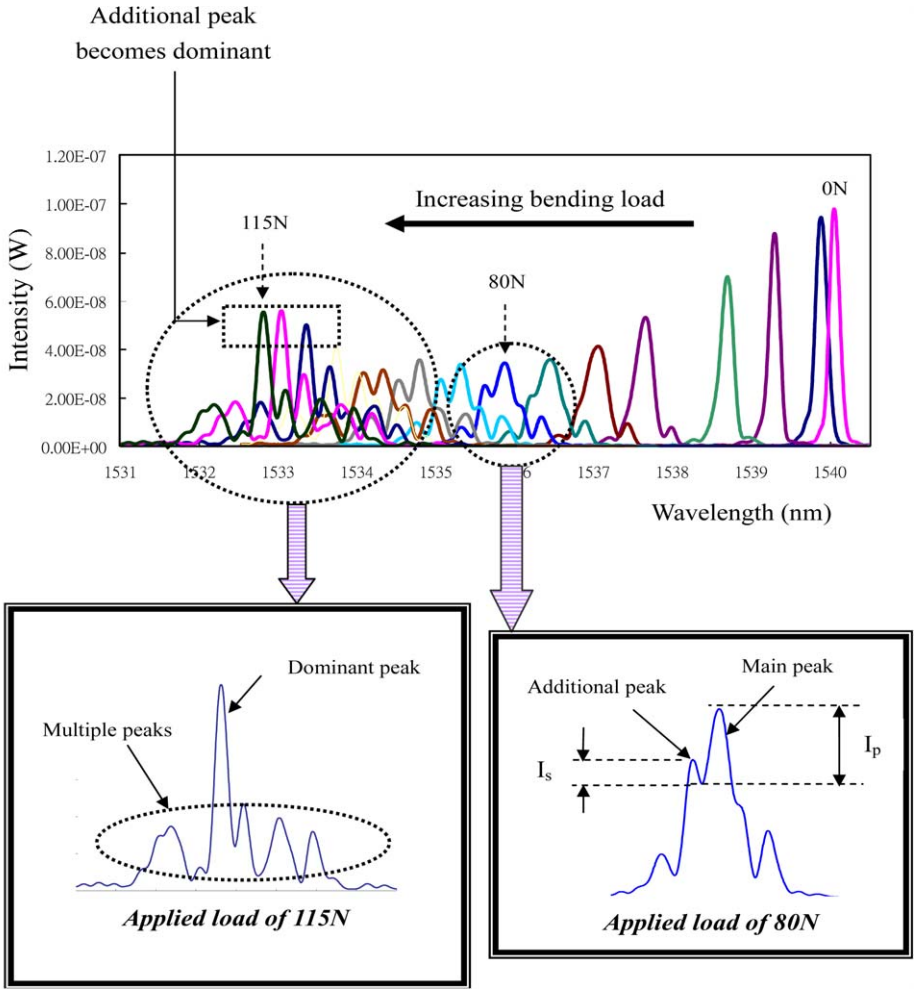

Fig. 3. Reflection spectra obtained from embedded FBG sensor in the intact case.

4. Results and discussion

4.1. Reflection spectrum

4.1.1. Intact specimen

Reflection spectra from the FBG sensor for intact beam with various bending loads are displayed in Fig. 3. The reflection spectrum shifts to the left with its original sharp narrow peak when an applied load is less than 80 N. By increasing the applied load, a concomitant increase in the Bragg wavelength shift and the bandwidth, as well as a decrease in the intensity of the reflection spectrum are obviously observed. Such a phenomenon can be explained by the bending effect within the gauge length of the FBG sensor. Likewise by increasing the bending load, the strain gradient along the grating is noticed to become higher, and then, the bandwidth increased and contrarily the intensity decreased. The Bragg wavelength shift is due to the average strain along the grating [11]. However, such a sharp peak starts to separate into multiple peaks while the applied load reaches to 80 N.

The presence of the multiple peaks can be characterized by defining the intensity ratio of the main and the additional peaks (i.e., $R_I = I_s/I_p$). In Fig. 3, it is observable that R_I increases with the load, and the additional peak becomes dominant just before the specimen fractured. Such an increase for the additional peak is believed due to the local strain concentration at a certain point of the grating. More multiple peaks, apart from such two peaks, are noticed as the applied load attains to its maximum, possibly owing to the chirped effect of the grating suppressed by the quadratic strain field in this case [12]. Right before the fracture of the beam, a dominant peak is observed among the multiple peaks because of the breakage of an optical fibre.

4.1.2. Delaminated specimen

In the case of the beam with a mid-plane delamination, reflection spectra from the FBG sensor are plotted in Fig. 4. The Bragg wavelength is noticed to decrease with the increasing compressive load at the beginning, similar with the way for the intact case. However, the intensity drops and rises in a fluctuating manner before the distortion occurs in the reflection spectrum. As the intensity is mainly dependent on the strain gradient along the grating, the change in the intensity indicates the interruption of the strain gradient owing to the existence of delamination. Concerning the shape of peaks in the reflection spectrum, a small additional peak shows up and arises at the left of the main peak under an applied load of 50 N. Compared

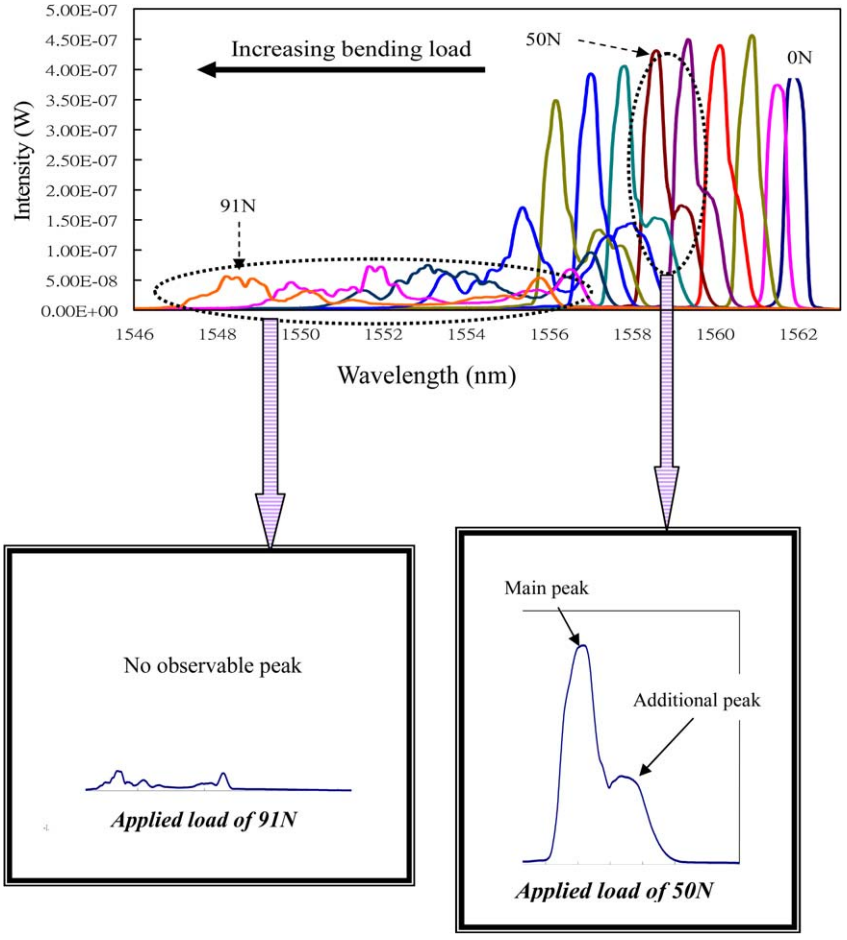

Fig. 4. Reflection spectra obtained from embedded FBG sensor in delaminated case.

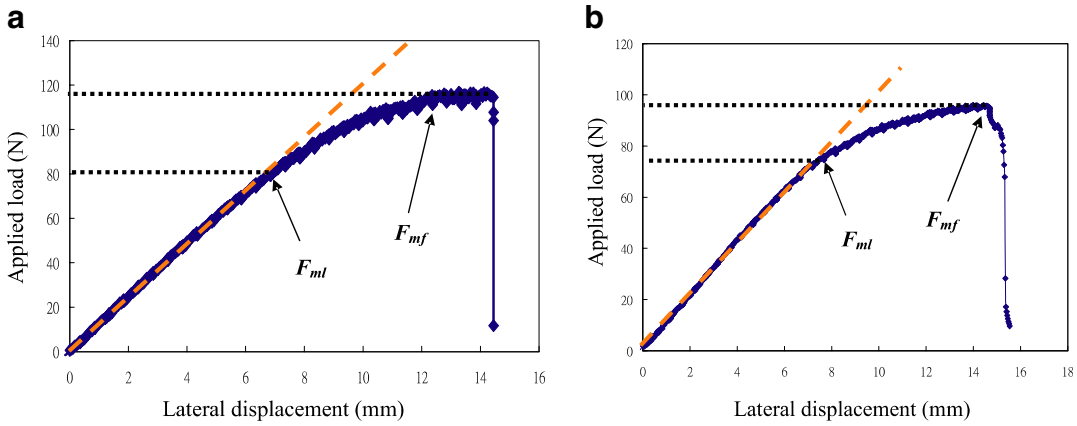

Fig. 5. Graph of applied load against the lateral displacement of the specimen in the (a) intact and (b) delaminated cases.

with the additional peak observed in the intact case, such a small peak is because of the stress concentration at the tip of delamination instead of a high strain gradient.

In addition, no dominant peak is observed in the last measurable reflection spectrum under 91 N. It is reasonable to interpret that the grating experienced an even strain distribution rather than a localized stress concentration at that moment. By considering the whole fracture process of the specimen, the overall pattern of the reflection spectra in this case looks similar with the one for the intact case when the applied load is small. However, it is totally different from the one in the intact case as the applied load is higher, as seen in Figs. 3 and 4.

4.2. Load–displacement relation and fracture monitoring

The load–displacement relation for the intact and delaminated cases under the ENF test is graphed in Figs. 5(a) and (b), with the similar trend. In the present study, F_{ml} and F_{mf} were defined as a maximum load for the validity of the linear elastic mechanical behaviour and a fractured load of the specimen, respectively, as highlighted in the figures. The macroscopic observation of the fractured ENF specimens is photographically illustrated in Fig. 6.

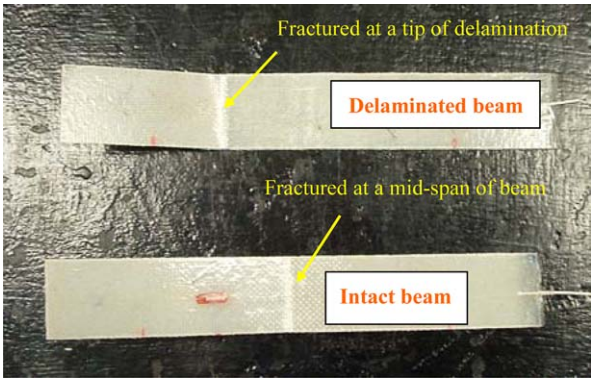

Fig. 6. A photograph of fractured intact and delaminated beams.

4.2.1. Intact specimen

The split of the main peak in the reflection spectrum, Fig. 3, can be explained by the load–displacement graph of the intact case. Referring to Fig. 5(a), F_{ml} is nearly equivalent to 80 N. Exceeding the applied load of 80 N, the stiffness of the beam varies with the increasing load rather than a constant value because of its non-linear elastic mechanical behaviour. Such a stiffness variation may interrupt the strain distribution along the grating, and hence accordingly cause the split of the main peak in the reflection spectrum. As a result, the split of the main peak is able to give an indication of the elastic limit of the composite beam. As the reflection spectrum at 115 N is still measurable in correspondence with F_{mf} of 115 N, it is evident that the FBG sensor still can give a response to the fracture process of the specimen until the specimen was totally fractured.

4.2.2. Delaminated specimen

Based on the load–displacement graph of the delaminated case, as plotted in Fig. 5(b), F_{ml} and F_{mf} of the specimen are 75 N and 96 N, respectively. The main peak disappears suddenly after the applied load reaches 91 N as indicated in Fig. 4. Disappearance of the main peak may be attributed to the appearance of damage at the grating region of the optical fibre. Referring to the fractured specimen observation under the delaminated case, as depicted in Fig. 6, the final fractured position is at the tip of the delamination instead of the mid-span of the beam. Therefore, the fibre breakage may lead to the additional stress concentration on the grating and eventually cause the fracture of the optical fibre.

5. Conclusion

Utilization of the embedded FBG sensors for monitoring mode II fracture behaviour of the GP/EP composite beam with a mid-plane delamination was demonstrated. In the ENF test, the FBG sensor showed its capability of sensing the non-uniform strain distribution around the

delamination tip. By virtue of the reflection spectrum from the FBG sensor, the fracture process of the specimens was characterized in terms of the Bragg wavelength shift, the bandwidth and the intensity of the reflection spectrum. It was concluded that the bandwidth of the reflection spectrum increase, while the corresponding intensity and the Bragg wavelength decreases with the increase of compressive load. Moreover, the presence of the additional peaks was highly correlated with the load-displacement graph captured from the ENF test.

Acknowledgement

This research project was funded by The Hong Kong Polytechnic Research Grant A-PF34.

References

[1] Walker L. Real time structural health monitoring – is it really this simple? International SAMPE Technical Conference, SAMPLE 2004. 2004. p. 1901–04.

[2] Thomson P, Marulanda JC, Marulanda JA, Caiceddo J. Real time health monitoring of civil infrastructures systems in Colombia. Proc SPIE 2001;4337:113–21.

[3] Choi MY, Kang KK, Kim JW, Park HY. The real-time health monitoring system of a large structure based on non-destructive testing. Proc SPIE 2003;5047:386–91.

[4] Leng JS, Asundi A. Non-destructive evaluation of smart materials by using extrinsic Fabry–Perot interferrometic and fibre Bragg grating sensors. NDT & E Int 2002;35:273–6.

[5] Ling HY, Lau KT, Cheng L, Jin W. Fibre optic sensors for delamination identification in composite beams using a genetic algorithm. Smart Mater Struct 2005;14:287–95.

[6] Takeda S, Okabe Y, Takeda N. Delamination detection in CFRP laminates with embedded small-diameter fiber Bragg grating sensors. Composites Part A 2002;33:971–80.

[7] Takeda S, Okabe Y, Yamamoto T, Takeda N. Detection of edge delamination in CFRP laminates under cyclic loading using small-diameter FBG sensors. Compos Sci Technol 2003;63(13):1885–94.

[8] Okabe Y, Tashiro S, Kosaka T, Takeda N. Detection of transverse cracks in CFRP composites using embedded fiber Bragg grating sensors. Smart Mater Struct 2000;9:832–8.

[9] Othonos A, Kalli K. Fiber Bragg gratings: fundamentals and applications in telecommunications and sensing. Boston, London: Artech House; 1999.

[10] Peters K, Studer M, Botsis J, Iocco A, Limberger H, Salathe R. Embedded optical fiber Bragg grating sensor in a nonuniform strain field: measurements and simulations. Exp Mech 2001;41(1):19–28.

[11] Huang S, LeBlanc M, Ohn MM, Measures RM. Bragg intragrating structural sensing. App Opt 1995;34(22):5003–9.

[12] Prabhugoud M, Peters K. Modified transfer matrix formulation for Bragg grating strain sensors. J Lightwave Techol 2004;22(10):2302–9.